THE ASTROPHYSICAL JOURNAL, 346:991–996, 1989 November 15

R AQUARII: EVIDENCE FOR A TWO-SIDED RADIO JET AND A CIRCUMBINARY SiO MASER

M. KAFATOS
Department of Physics, George Mason University
J. M. HOLLIS
Space Data and Computing Division, NASA/Goddard Space Flight Center
F. YUSEF-ZADEH[1,2] AND A. G. MICHALITSIANOS
Laboratory for Astronomy and Solar Physics, NASA/Goddard Space Flight Center
AND
M. ELITZUR
Department of Physics and Astronomy, University of Kentucky
Received 1988 November 7; accepted 1989 May 17

ABSTRACT

We have detected collimated 4.86 GHz (~6 cm) radio continuum emission southwest (SW) of the symbiotic variable R Aquarii by combining data corresponding to different configurations of the Very Large Array (VLA). In the context of a previously reported northeast (NE) 6 cm jet structure, the orientation of the newly found SW radio structure suggests bipolar symmetry, extending to distances of ~2500 AU on either side of the central H II region. The amorphous morphology of the new collimated SW structure is distinct from the discrete radio knots NE of the central object. Further, we have determined the radio spectral index distribution between 2 and 6 cm for nearly all of the radio features found in R Aquarii. Additionally, we have detected 14.94 GHz (~2 cm) continuum emission at the SiO maser position which is located ~250 AU away from the binary system whose orbital semimajor axis is ~17 AU. This provides further evidence that the maser-emitting region is far removed from the system's Mira envelope and may well be due to local shock phenomena in the circumbinary nebulosity. The implications concerning the newly detected bipolar 6 cm structure, the spectral index gradient of the NE jet structure, and the 2 cm emission component at the SiO maser location are described in context of a thick accretion disk model that has been previously proposed to explain the morphology and kinematics of the R Aquarii radio/optical jet.

Subject headings: masers — nebulae: H II regions — stars: circumstellar shells — stars: individual (R Aqr) — stars: radio radiation — stars: symbiotic

I. INTRODUCTION

One of the most interesting classes of binary objects is the symbiotic star system, and the closest one to Earth is R Aquarii (250 pc, according to Whitelock 1987) which, by virtue of proximity, is often observed and analyzed as a prototypical dust-type symbiotic system (see Michalitsianos and Kafatos 1988 and references therein). These systems are suspected to be comprised of a hot subdwarf companion in orbit around a cool, voluminous, red giant star whose light varies, in the case of R Aquarii, with a 387 day period. It is believed that material lost from the cool star is captured by the hot star predominantly at periastron, forming an accretion disk which can eject material in both directions parallel to the disk axis.

In 1980 a brilliant jet of material was discovered by optical means (Herbig 1980) emanating from R Aquarii toward the NE; in 1982 Sopka *et al.* (1982) detected the optical jet's 6 cm radio counterpart. The radio/optical jet extends ~10″ NE of R Aquarii, but the existence of a definitive radio counterjet toward the SW has eluded detection. Indeed, there has always been some question as to whether the term "jet" should be applied to the R Aquarii NE radio/optical features. In order to make a sensitive measurement for detecting a SW counterpart to the NE radio structure, we combined all of the 6 cm radio data acquired with the VLA since 1982, by using data obtained at several array configurations.

Our efforts were rewarded by the detection of a collimated, amorphous radio continuum structure, which extends ~10″ SW of R Aquarii, and is best seen in radio maps with spatial resolutions ≥ 2″ constructed from the combined data set. This detection of a SW jet provides strong evidence for a symmetrical or bipolar jet phenomenon when interpreted in context with the less amorphous, collimated NE jet structure. We suggest that the bipolar appearance of the radio structure provides further evidence for collimated mass outflow in the system due to a geometrically thick accretion disk which, via radiation pressure, expells material in both directions normal to the plane of disk, primarily at periastron passage. It may well be that the accretion disk is inclined relative to the plane of the binary orbit (Kafatos, Michalitsianos, and Hollis 1986). As such, the extended Mira atmosphere could partially obstruct the collimated flow on the side of the disk facing the M giant, creating turbulent motions, which might explain the amorphous morphology of the less intense SW jet counterpart.

We also were motivated to search for a 6 cm radio continuum counterpart to SiO maser emission by making images with the combined data set at the highest possible resolution of ~0.″5, typical of the A-configuration. Such small-scale features might be associated with SiO maser emission detected in the system; moreover, Hollis *et al.* (1986) had previously deter-

[1] National Research Council Resident Research Associate.
[2] On leave from Northwestern University.

mined the position of the centroid of the R Aquarii SiO maser emission which is presumably composed of several spots. This position is far removed from the atmosphere of the system's Mira variable and, thus, indicates that the maser is formed in the circumbinary nebulosity. Thus, we also obtained 2 cm continuum observations in the A/B-configuration, which is comparable in resolution to 6 cm observations in the A-configuration, to specifically probe south of the R Aquarii central H II region at the location of SiO maser emission. Although our 6 cm images failed to show discrete emission, the 2 cm observations reveal at least two discrete knots near the SiO position. If these continuum knots engulf the SiO maser spots, the maser emitting regions are smaller than the limiting VLA resolution at 6 cm.

Our observations and details of data reduction and analysis are given in the next section. The importance of this work in context with the SiO maser and jet phenomena in general is discussed in § III.

II. OBSERVATIONS AND DATA REDUCTION

a) 6 Centimeter Continuum Observations

New continuum 6 cm observations of R Aquarii were obtained with the NRAO[3] VLA in the A-configuration and were combined with previously reported 6 cm observations taken in the B-configuration (two 8 hr observing sessions described in Kafatos, Hollis, and Michalitsianos 1983 and Hollis *et al.* 1985) and the D-configuration (one 8 hr observing session described in Hollis *et al.* 1987).

The new 6 cm configuration VLA observations of R Aquarii reported in this work were made between 2000 and 0400 LST, beginning on 1987 September 22. Twenty-six antennas were employed at 6 cm (nominally 4,860 MHz), utilizing an intermediate frequency (IF) bandwidth of 50 MHz and two IF pairs separated by 50 MHz. Spacing between antennas varied between 0.8 and 36.6 km. The phase center of the observations was at the nominal position of R Aquarii, which for epoch 1950.0 in equatorial coordinates is $\alpha = 23^h41^m14^s.269$ and $\delta = -15°33'42''.890$, or in galactic coordinates $l = 66°.5$ and $b = -70°.3$. Observations of R Aquarii were interleaved with observations of 2345−167 for phase calibration purposes. On-source integration time (exclusive of the array move time) for R Aquarii and 2345−167 totalled 357 and 55 minutes, respectively. Observations of 3C 48 were made to establish the flux calibration scale for R Aquarii and 2345−167 by assuming 3C 48 has constant 6 cm flux densities of 5.59/5.64 Jy for the IF pairs. For the observational epoch, the IF pair bootstrapped 6 cm fluxes of 2345−167 were 2.189 ± 0.008/2.132 ± 0.009 Jy. The calibrated amplitudes and phases for the two IF pairs for the R Aquarii observations were combined to achieve a $2^{1/2}$ enhancement in signal to noise, were self-calibrated in order to minimize the antenna-based phase errors, and were then Fourier-transformed before CLEANing (a particular method of sidelobe removal; cf. Clark 1980) the spatial maps.

The 6 cm data from all observing runs in the A-, B-, and D-configurations were combined to obtain radio maps which are based on sampling over a wide range of spatial frequencies. We applied a self-calibration procedure (ASCAL in AIPS) which minimizes the antenna-based phase errors of individual data sets corresponding to different configurations. The data sets were then combined one at a time before a global self-calibration was applied. The combined data sets were very effective in enhancing weak and extended source structures which were not obtainable in previous studies of a data set belonging to a single configuration.

Figure 1 shows the R Aquarii continuum emission within 5″ of the central H II region at the highest resolution obtainable from these data sets; the 6 cm beam is 0″.48 × 0″.33 and results from uniformly weighted u, v data points, or baseline pairs. The weighting is uniform in the sense that each baseline, regardless of the number of data points taken at that baseline, receives equal weight. An improved sensitivity to extended structure was achieved in constructing Figure 2, where the u, v data points were naturally weighted (i.e., each observing data point received equal weight); the resultant synthesized 6 cm beam is 2″.33 × 1″.39. With a field of view of 40″, Figure 2 shows the complexity of the new SW feature B′ which is clearly a counterpart to previously reported NE feature B (Sopka *et al.* 1982); also seen in Figure 2 is the prominent central H II region and the suggestion of a weakly emitting radio structure associated with feature A. Using the same data set employed in the construction of Figures 1 and 2, Figure 3 is generated by weighting the u, v data points with a 30 kλ Gaussian taper function across the projected baselines; the resultant synthesized 6 cm circular beam is 4″.49. As seen in Figure 3, application of this tapering brings out the extended emitting features at the expense of diluting the compact and discrete sources and, as such, smooths and enhances the distribution of weak, low-level structure in both features B and B′. Figure 3 clearly shows that

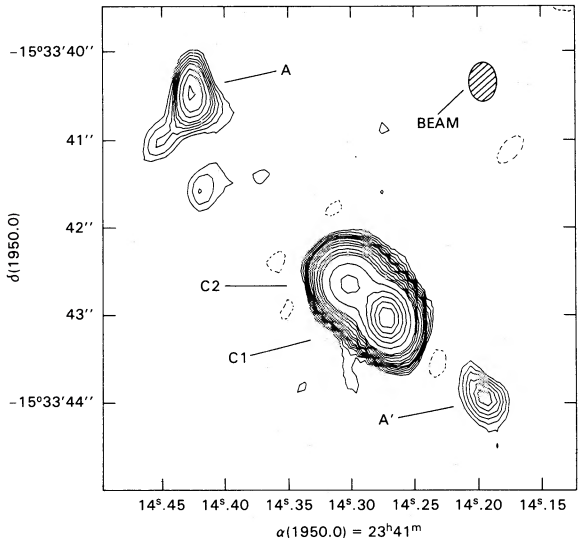

FIG. 1.—A 6 cm contour plot of a uniformly weighted image of the inner jet components of the R Aquarii binary system using VLA data taken in the A-, B-, and D-configurations with a resulting resolution of 0″.48 × 0″.33. At this plot scale, the entire binary system itself resides within the confines of the central H II region feature C1 (Michalitisianos *et al.* 1988) whose peak flux is ~3.89 mJy beam^{-1}. Contour levels shown are −3, 3, 4, 5, 6, 7, 8, 10, 12, 15, 20, 25, 30, 50, 75, 100, 125, and 150 multiples of the rms map noise level which is 22.7 μJy beam^{-1}. Note the highly suggestive bow shock morphology of feature A. A′ shown here is completely resolved (cf. Hollis *et al.* 1985). It can be seen that the centroid of SiO maser emission spots at position 14ˢ.277(10) and 44″.0(2), as determined by Hollis *et al.* (1986), is not coincident with any significant discrete 6 cm continuum emission (cf. Fig. 4). Larger scale features, such as B and B′ shown subsequently in Figs. 2 and 3, cannot be readily seen at the resolution of this figure and, therefore, are not included in the field of view.

[3] The National Radio Astronomy Observatory is operated by Associated Universities, Inc., under cooperative agreement with the National Science Foundation.

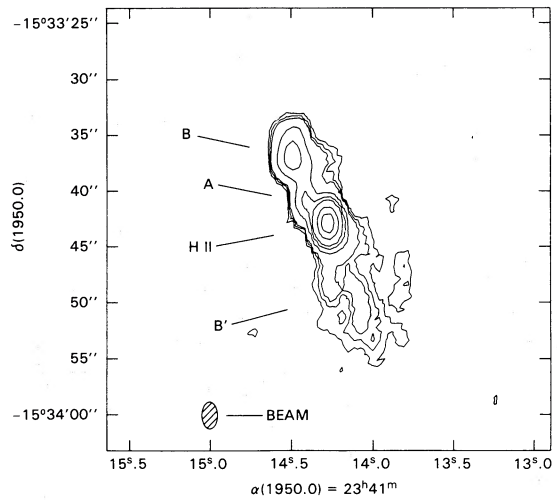

FIG. 2.—A 6 cm contour plot of a naturally weighted image of the R Aquarii jet using VLA data taken in the A-, B-, and D-configuration with a resulting resolution of 2".33 × 1".39. The central H II region (so marked) has a peak flux of 7.25 mJy beam^{-1}. Contour levels shown are 5, 7.5, 10, 30, 60, 100, 250, and 450 multiples of the rms map noise level of 11.2 μJy beam^{-1}. Smaller scale features, such as C2 and A′ shown in Fig. 1, cannot be readily seen at this resolution; however, A can be inferred by a NE protrusion emanating from (and in proximity to) the central H II region. Radio feature B was discovered in 1982 (Sopka *et al.* 1982), and this work now has detected its counterpart, feature B′, which is weaker in integrated flux by a factor of ~1.5 and appears more amorphous than B.

the global properties of B and B′ are similar morphologically and opposite one another in position angle relative to the central H II region. At this point we emphasize that the dynamic range achieved in Figures 1, 2, and 3 is ~170, 650, and ~300, respectively; this achievement is quite remarkable for such a weak radio source (see Table 1 fluxes).

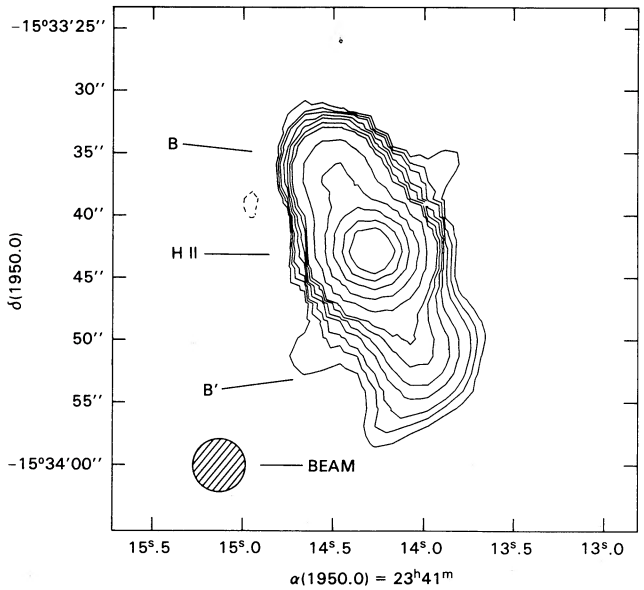

FIG. 3.—A 6 cm contour plot of a 30 kλ tapered image of the R Aquarii jet using VLA data taken in the A, B, and D configurations with a resulting resolution of 4".49. The central H II region (so marked) has a peak flux of 8.86 mJy beam^{-1}. Contour levels shown are −3, 3, 4, 5, 7, 9, 12, 15, 30, 60, 100, 150, and 200 multiples of the rms map noise level of 29.3 μJy beam^{-1}. Only B and its counterpart B′ can be seen flanking the central H II region (see legends to Figs. 1 and 2).

TABLE 1

INTEGRATED 6 CENTIMETER AND 2 CENTIMETER FLUXES AND POSITION ANGLES OF RADIO FEATURES DISPLAYED IN THE IMAGERY OF FIGURES 1–4

Feature (1)	6 cm Flux (mJy) (2)	2 cm Flux (mJy) (4)	Position Angle (5)	Notes (6)
B	2.3	...	~29°	1, 2
A	0.6	0.8	~45	1, 3
C2	3.2	...	~55	1, 3, 4
C1 + C2	...	10.0	...	1, 3, 4
C1	4.9	...	...	1, 3, 4
A′	0.2	...	~231	1, 5
S1	...	0.9	~170	1, 6
S2	...	1.4	~190	1, 6
B′	1.5	...	~209	1, 2

NOTES.—(1) The 1 σ error on the flux is estimated to be 10%–20% of the tabulated value. (2) B and B′ cannot be detected at 2 cm with the VLA hybrid A/B configuration. (3) See the pixel-for-pixel spectral index image of this feature (Fig. 5). (4) The 6 cm data resolve C1 and C2, but these features are severely blended in 2 cm data. (5) A′ is not apparent in the 2 cm data, thus suggesting a negative spectral index for this feature. (6) S1 and S2 are not apparent in the 6 cm data, thus suggesting positive spectral indices for these features.

b) 2 Centimeter Continuum Observations

Continuum 2 cm observations of R Aquarii were obtained with the NRAO VLA in the hybrid A/B configuration between 0000 and 0400 LST on 1987 November 4 and between 2200 and 0230 LST on 1987 November 7. Twenty-six antennas were employed at 2 cm (nominally 14,940 MHz), utilizing an IF bandwith of 50 MHz and two IF pairs separated by 50 MHz. Spacing between antennas varied between 0.3 and 22.8 km. For the 2 cm observations, we used the same phase center and observational methods as were employed in the 6 cm observations. On-source integration time (exclusive of array move time) for R Aquarii and 2345−167 totalled 367 and 55 minutes, respectively. Flux calibration observations of 3C 48 were made, assuming that 3C 48 has a constant 2 cm flux density of 1.85 Jy for both IF pairs. For the observational epochs, the IF pair bootstrapped 2 cm fluxes of 2345−167 were 1.858 ± 0.021/1.865 ± 0.018 Jy on 1987 November 4 and were 1.889 ± 0.015/1.879 ± 0.014 Jy on 1987 November 7.

With a 550 kλ Gaussian taper applied to the 2 cm data, the resulting synthesized beam is 0".46 × 0".27, and the image corresponding to this resolution is shown in Figure 4. As can be seen, there are two discrete features (S1 and S2) south of the central H II region in the vicinity of the SiO maser position whose positional uncertainty is indicated by 1 σ error bars. The 2 cm data of Figure 4 and the 6 cm data of Figure 1 can be directly compared because both are at similar resolutions. However, the rms noise level is 4 times better in the 6 cm image than the 2 cm image. The 6 cm data of Figure 1 do not show S1 and S2; conversely the 2 cm data of Figure 4 do not show feature A′. This (see Table 1 flux, F, values) argues for a negative spectral index, α, for feature A′ and positive spectral indices for features S1 and S2, using the convention $F \propto \nu^{\alpha}$, where ν is the observational frequency. Quite probably S1 and S2 are optically thick and thermal, while A′ is likely nonthermal.

In order to quantitatively compare the 6 cm and 2 cm images, we convolved both images with a slightly larger beam (i.e., 0".49 × 0".34) and made a spectral index image shown in Figure 5. The central H II region C1 shown in Figure 5 is optically thick and thermal as one expects for a stellar wind

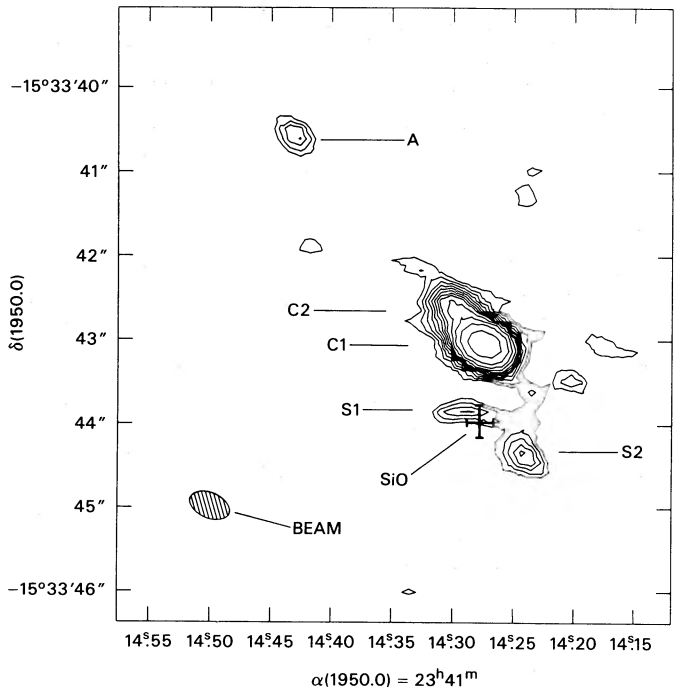

FIG. 4.—A 2 cm contour plot of a 550 kλ tapered image of R Aquarii using VLA data taken in the hybrid A/B-configuration with a resulting resolution of 0.″46 by 0.″27; this beam size is comparable to that of the 6 cm data (Fig. 1). Here we see the central H II region (C1), whose peak flux is ~3.98 mJy beam^{-1}, with a protrusion to the NE which is due to feature C2 and outlying feature A. Contour levels shown are 3, 4, 5, 6, 7, 8, 9, 10, 12, 15, 20, and 30 multiples of the rms map noise level which is 88.4 μJy beam^{-1}. Toward the south of the central H II region, newly detected continuum features S1 and S2 are shown with the position of the centroid of SiO maser emission plotted for reference (Hollis *et al.* 1986); these features are not seen in the 6 cm data (Fig. 1), indicating that their radio spectra are probably thermal, optically thick and due to shock-wave heating of the circumbinary nebulosity.

($\alpha \sim +0.6$ for a spherically symmetric steady state ideal case), while nearby NE jet feature C2 is slightly nonthermal. As one moves further out the NE jet to A, the spectral index is typical of an optically thick, thermal region. At the NE jet extremity (feature B in Fig. 2), the spectral index is nearly zero (Hollis *et al.* 1985) which indicates an optically thin, thermal source. Hence, the spectral index distribution or gradient of the NE jet is quite complex but largely thermal in nature.

III. DISCUSSION AND CONCLUSIONS

a) The Symmetrical Jet

Relative to the central H II region, symmetrical, collimated features B and B′ extend to a distance of ~2500 AU on opposite sides of the central object, assuming a distance to R Aquarii of 250 pc. This morphology, which is shown in Figures 2 and 3, provides strong evidence for bipolar mass ejection from the system (cf. Kafatos and Michalitsianos 1982; Hollis *et al.* 1985; Kafatos, Michalitsianos, and Hollis 1986). Moreover, the spectral index gradient of the NE jet, as one proceeds outward from the optically thick, thermal feature C1 (central H II region), suggests that the origin of the jet (i.e., C2) is nonthermal emission probably produced by synchrotron emission from a mildly relativistic gas. Farther out, the spectrum changes to thermal for outlying features A (optically thick) and B (optically thin). From ultraviolet observations and analysis it is found that features C2 and A are higher in excitation than feature B because they are closer to the source of ionization which is presumably the radiation cone emanating from the accretion disk (see Kafatos, Michalitsianos, and Hollis 1986 and arguments to follow); moreover, since the ultraviolet observations indicate that C2 and A were initially formed, ionized, and accelerated at the accretion disk surface ($T_{\rm inner} \sim 10^5$ K), they are also hotter than the central H II region C1 which is not directly exposed to the high-energy radiation because it is largely being shielded by the thick accretion disk. This result is obtained from observations taken with the *International Ultraviolet Explorer* satellite which indicate that the highest excitation emission lines observed in the R Aquarii system appear to be located immediately NE of the central star. Further, R Aquarii is known to be a soft X-ray source, but the spatial distribution for this type emission has not yet been determined (Viotti *et al.* 1987).

The radio emission SW of R Aquarii (see contours in Figs. 2 and 3) indicates a more amorphous structure compared with the knots of discrete sources, as seen in Figure 1, NE of the central H II region. As listed in Table 1, flux values indicate that SW counterjet features A′ and B′ are weaker than the corresponding NE features A and B by factors of ~3 and ~1.5, respectively. The foregoing suggests that corresponding jet/counterjet features tend to become comparable in intensity with increasing distance from the central star and both the jet and counterjet eventually blend with the overall nebulosity of the NS nebula. For an electron temperature $T_e \sim 10^4$ K, we estimate that the electron density range for the knotty NE jet and the more amorphous SW counterjet is $n_e \sim 10^3$–10^4 cm^{-3}; these densities imply a cooling time scale range of 7–0.7 yr, respectively. Such short cooling times and the seeming stability of the NE jet over several years (Hollis *et al.*

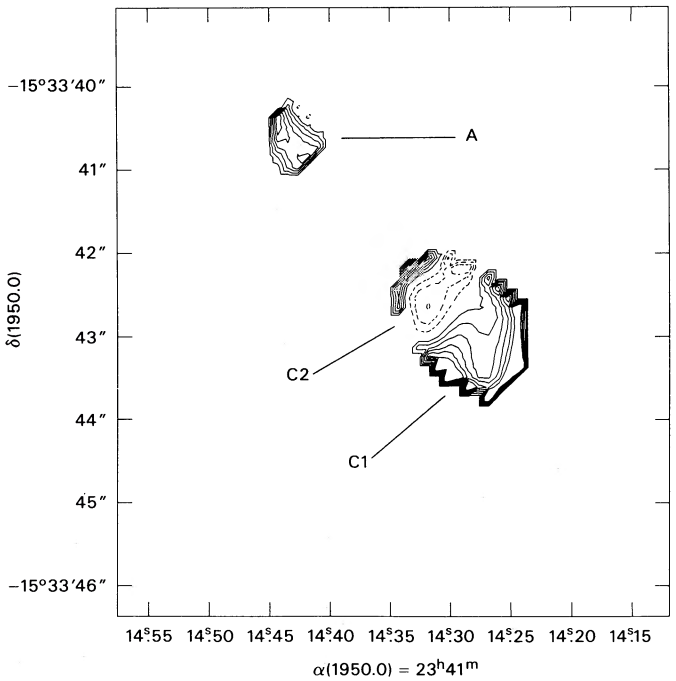

FIG. 5.—A contour plot of the spectral indices of features C1, C2, and A derived from data in Fig. 1 (6 cm data) and Fig. 4 (2 cm data). Contour levels shown are −0.3, −0.2, −0.1, +0.1, +0.2, +0.3, +0.4, +0.5, and +0.6 spectral index values. Clearly feature C2 is nonthermal, while features C1 and A are optically thick and thermal (see text).

1985) require that the NE and SW jets be continually heated. The heating is likely accomplished in the following manner: the jet/counterjet features are bathed in two cones of ultraviolet radiation emergent from both sides of a thick accretion disk which surrounds the hot companion to the Mira variable (Kafatos, Michalitsianos, and Hollis 1986).

b) The SiO *Maser and Coincident Radio Continuum Emission*

There is independent evidence of even greater differentiation in densities inferred from the SiO masing process in R Aquarii (Hollis *et al.* 1986). The binary star system R Aquarii is unique because it is the only symbiotic which exhibits SiO maser emission. Except for R Aquarii and Omicron Ceti (Mira), all other, SiO masers observed so far in the galaxy are associated with either a singly evolving late-type or pre–main-sequence star. The mere fact that an SiO maser exists, occurring in the excited vibration state of the molecule, implies both high densities and high temperatures in the region. Independent of the specific details of the pump, every pumping scheme proposed so far requires that SiO $v = 1$–0 vibration transition be optically thick. This implies SiO column densities in excess of $\sim 10^{18}$ cm^{-2}. Likewise, to support a significant population of SiO in the $v = 1$ state, which is ~ 1750 K above the ground state, the temperature must be at least ~ 1000 K; at the same time, however, the temperature in the maser region cannot exceed ~ 2500 K to avoid dissociation of the gas phase SiO molecules.

The required high densities in an otherwise rather rarefied region are most likely the result of shock compression of a clump of material running into the ambient gas. The shock heating can also provide the high temperatures required for the SiO excitation and is expected to produce continuum radio emission. It is therefore highly significant that we detected two clumps (S1 and S2) of 2 cm emission south of R Aquarii, as evident in Figure 4, near the position of the SiO maser emitting region (see Hollis *et al.* 1986). The existence of S1, S2, and the SiO maser south of the central H II region provides support for the hypothesis that these southern features are shielded from an intense bath of radiation arising from the central ionizing source. The detection of S1 and S2 and the fact that each are unresolved place an upper limit of 2×10^{15} cm for the diameter of the SiO maser region. Assuming level populations roughly in accord with a Boltzmann distribution at 2500 K, the optical depth of the SiO $v = 1$–0 transition is

$$\tau_{v=1-0} = 1.3 \times 10^{-24} n_{\rm H} L \chi_{\rm SiO} \Delta v^{-1} , \quad (1)$$

where $n_{\rm H}$ (cm^{-3}) is the hydrogen density, L (cm) is the pathlength of the SiO emitting region, Δv (km s^{-1}) is the linewidth, and $\chi_{\rm SiO}$ is the fraction of silicon in SiO (e.g., Elitzur 1980). Here we assumed a cosmic silicon abundance, namely Si/H = 3×10^{-5}. Thus, with $\Delta v \sim 3$ km s^{-1} (Hollis *et al.* 1986), $\chi_{\rm SiO} = 1$, and $L \leq 10^{15}$ cm, we find $n_{\rm H} \geq 2 \times 10^9$ cm^{-3}. The upper limit on the maser size shows that its dimension could be similar to the observed spot sizes in late-type stars of $\sim 10^{13}$–10^{14} cm (Lane 1982). The densities would then be comparable to those inferred for late-type SiO maser stars, $\sim 10^{10}$–10^{11} cm^{-3} (Elitzur 1980). These foregoing estimates are consistent with the S1 and S2 2 cm radio emission detected; because these clumps have no 6 cm counterpart in Figure 1, they in all likelihood have positive spectral indices and, thus, are optically thick and thermal. Hence, for optically thick free-free emission, we have the following relation:

$$n_{\rm H}^2 \chi_{\rm H}^2 T^{-0.5} L^3 \geq 2.6 \times 10^{53} \text{ cm}^{-3} \text{ K}^{-0.5} , \quad (2)$$

where $\chi_{\rm H} \equiv n_e/n_{\rm H}$ allows for the hydrogen to be partially ionized. Indeed, if the parameters inferred from the SiO maser emitting region are used, this relation is obeyed by a comfortable margin for any reasonable estimate of $\chi_{\rm H}$ (~ 0.1, say). It is entirely possible that the emitting regions are arranged in layers or shells as a result of the shock compression with the radio emitting region somewhat thinner than the interior SiO emitting layer.

The requisite densities in the SiO-emitting region (i.e., $\geq 2 \times 10^9$ cm^{-3}) imply a lower limit shock speed range of 150 km s^{-1} (for a molecular preshock gas) to 1500 km s^{-1} (for a pure H II gas) if no magnetic fields are present and if the jet component ambient densities are $\sim 10^5$ cm^{-3} (see Kafatos, Michalitsianos, and Hollis 1986). If the density in the maser region is as high as $\sim 10^{11}$ cm^{-3} (Elitzur 1980), then the aforementioned shock speed range would increase by a factor of ~ 7. Such speeds are high compared to the speeds deduced from optical spectra (Solf and Ulrich 1985) but more favorably compare to the range allowed by the ultraviolet observations of C IV, which indicate the presence of a fast wind ($v_\infty \leq 10^3$ km s^{-1}, from Michalitsianos *et al.* 1988*a*), and Mg II, which indicate the presence of a slow wind ($v_\infty \sim 200$ km s^{-1}, from Johnson 1980). On the other hand, from theory we obtain $v_\infty \sim 6 \times 10^4$ km s^{-1} and an ambient density of 0.6 cm^{-3} for a spherical wind with a mass loss of $\sim 10^{-7}$ $M_\odot$ yr^{-1} (see Hollis *et al.* 1985). Thus, the observations (Hollis *et al.* 1985) imply that a spherical wind cannot produce sufficient compression at ~ 250 AU to account for the observations herein. Hence, directional flow (i.e., a jet) likely accounts for the compression.

c) Application of Jet Models

R Aquarii is not only the nearest symbiotic star, but is the nearest astrophysical jet source. Thus, detailed investigations of the properties of the R Aquarii jet may provide important clues concerning jet phenomena in general. Moreover, it is difficult to understand the morphology of the jet in R Aquarii without invoking the existence of a thick accretion disk that is formed by tidal mass exchange between the extended atmosphere of the Mira variable and the hot companion (Kafatos, Michalitsianos, and Hollis 1986). The geometrically thick disk provides a natural explanation for the ejection of gas parcels along the jet/counterjet axis, and, because the disk is nearly edge-on to the line of sight (see Willson, Garnavich, and Mattei 1981), accounts for no observed stellar continuum from the hot companion. Further, the accretion disk, if precessing, could account for the regular progression of radio feature position angles (see Table 1). Analogous to the case of SS 433, one can estimate the relationship between the binary orbital period, $t_{\rm orb}$, the orbital period of the accretion disk, t_d, and the precessional period $t_{\rm prec}$, which is

$$t_d \times t_{\rm prec} \sim 3 \times t_{\rm orb}^2 \quad (3)$$

(Davidson and McCray 1980), where the disk period, $t_d = 2\pi \times r^{1.5}/(GM)^{1/2}$. From geometrical arguments of the eclipse of the Mira by, presumably, the cool outer regions of the thick accretion disk (Kafatos and Michalitsianos 1982), we estimate that the disk radius $r \sim 10^{13}$ cm. This accretion disk scale size is also required to provide sufficient radiative acceleration of the grains (Kafatos, Michalatsianos, and Hollis 1986). Moreover, from the variation of the position angles of the individual radio knots, Michalitsianos *et al.* (1988*b*) estimate that $t_{\rm prec} \sim 2000$ yr. Substituting these values in equation (3), we can solve for $t_{\rm orb}$. Assuming the mass of the compact star is ~ 1 $M_\odot$, we

find $t_{orb} \sim 20$ yr, which is within the range of the estimates of the binary orbit (cf. Merrill 1934, 1940, 1950; Willson, Garnavich, and Mattei 1981; Kafatos and Michalitsianos 1982; Wallerstein 1986). On the other hand, if precession of the accretion disk is not occurring, then the variation of position angles in Table 1 may reflect the vagaries of orbital motion; obviously *an orbit determination for this object would be extremely helpful but difficult, considering that the hot companion remains unseen at the present epoch.*

Since the prevalent properties of the jet/counterjet are largely thermal and can be approximated by cylindrical geometry, the power provided is

$$L = \pi/2 \times \rho_j v_\infty^3 l_j^2 , \quad (4)$$

where l_j is the cross sectional radius of the jet, ρ_j is the jet gas density, and v_∞ is the escape velocity of the jet (cf. Willis 1981). For R Aquarii, we assume $v_\infty \sim 100$ km s^{-1} (cf. Solf and Ulrich 1985). Taking the cross sectional radius of the jet to be in the range 10^{15}–10^{16} cm, appropriate for the various NE features, and a gas density in the range 10^3–10^4 cm^{-3}, which is probably a mean as evident from the counterjet/jet densities, we find from equation (4) that $2.5 \times 10^{30} \leq L \leq 2.5 \times 10^{33}$ ergs s^{-1}. This amount of power is more than capable of ionizing the large-scale diffuse NS nebula which extends some 30″ beyond both the SW and NE jet features even if the prevalent densities of the extended NS nebula are more than an order of magnitude less than those found for the jet components (e.g., $n_e \sim 10^4$ cm^{-3} for feature B).

The properties exhibited by the R Aquarii jet/counterjet structures are reminiscent of those found in extragalactic jets: (1) nonthermal emission; (2) double radio structure; (3) the existence of blobs or gas parcels as in M87 (Arp 1981); and (4) the morphological suggestion of precession as in the jet in 3C 273 (Arp 1981). Bridle (1985) has provided a criterion for one-sidedness or two-sidedness for an extragalactic jet: one-sided if the ratio of the intensities between the brighter and fainter components is >4 but two-sided otherwise. In this scheme, the R Aquarii jet would qualify as a double-sided jet because the ratio of intensities is $B/B' \sim 1.5$. We also emphasize that because the bulk motion velocities in R Aquarii are definitely nonrelativistic ($\sim$50–100 km s^{-1}; Solf and Ulrich 1985), relativistic beaming cannot possibly be a reason for the different intensities between the jet and counterjet components. The relativistic beaming mechanism still has problems for extragalactic jets primarily because of statistical arguments (Arp 1981), and also because relativistic bulk motion velocities have still not been unequivocably demonstrated in extragalactic jets (Willis 1981). For these reasons, the proximity of R Aquarii undoubtedly affords us a unique opportunity to probe jet phenomena in detail and such research may elucidate problems of extragalactic jets as well.

We thank Peggy Perley for help with the calibration of our VLA data sets. F. Y.-Z. appreciates the hospitality of the Space Data and Computing Division at NASA/GSFC where the image processing was accomplished. M. K. and J. M. H. appreciate and acknowledge the support of NASA contract NAS5-29310T and NASA RTOP 188–44–23 Task 01, respectively.

REFERENCES

Arp, H. 1981, in *Optical Jets in Galaxies* (ESA SP-162), ed. B. Battrick and J. Mort (Paris: ESO), p. 53.
Bridle, A. H. 1986, *Canadian J. Phys.*, **64**, 353.
Clark, B. G. 1980, *Astr. Ap.*, **89**, 377.
Davidson, K., and McCray, R. 1980, *Ap. J.*, **241**, 1082.
Elitzur, M. 1980, *Ap. J.*, **240**, 553.
Herbig, G. H. 1980, *IAU Circ.*, No. 3535.
Hollis, J. M., Kafatos, M., Michalitsianos, A. G., and McAlister, H. A. 1985, *Ap. J.*, **289**, 765.
Hollis, J. M., Kafatos, M., Michalitsianos, A. G., Olivesen, R. J., and Yusef-Zadeh, F. 1987, *Ap. J. (Letters)*, **321**, L55.
Hollis, J. M., Michalitsianos, A. G., Kafatos, M., Wright, M. C. H., and Welch, W. J. 1986, *Ap. J. (Letters)*, **309**, L57.
Johnson, H. M. 1980, *Ap. J.*, **237**, 840.
Kafatos, M., Hollis, J. M., and Michalitsianos, A. G. 1983, *Ap. J. (Letters)*, **267**, L103.
Kafatos, M., and Michalitsianos, A. G. 1982, *Nature*, **298**, 540.
Kafatos, M., Michalitsianos, A. G., and Hollis, J. M. 1986, *Ap. J. Suppl.*, **62**, 853.
Lane, A. P. 1982, Ph.D. thesis, University of Massachusetts, Amherst.
Merrill, P. W. 1934, *Ap. J.*, **81**, 312.
Merrill, P. W. 1940, *Spectra of Long Period Variable Stars* (Chicago: University of Chicago Press), p. 82.
———. 1950, *Ap. J.*, **112**, 514.
Michalitsianos, A. G., and Kafatos, M. 1988, in *The Symbiotic Phenomenon*, ed. J. Mikolajewska *et al.* (Dordrecht: Kluwer), p. 235.
Michalitsianos, A. G., Kafatos, M., Fahey, R. P., Viotti, R., Cassatella, A., and Altamore, A. 1988*a*, *Ap. J.*, **331**, 477.
Michalitsianos, A. G., Oliversen, R. J., Hollis, J. M., Kafatos, M., Crull, H. E., and Miller, R. J. 1988*b*, *A.J.*, **95**, 1478.
Solf, J., and Ulrich, H. 1985, *Astr. Ap.*, **148**, 274.
Sopka, R. J., Herbig, G., Kafatos, M., and Michalitsianos, A. G. 1982, *Ap. J. (Letters)*, **258**, L35.
Viotti, R., Piro, L., Freidjung, M., and Cassatella, A. 1987, *Ap. J. (Letters)*, **319**, L7.
Wallerstein, G. 1986, *Pub. A.S.P.*, **98**, 118.
Whitelock, P. A. 1987, *Pub. A.S.P.*, **99**, 573.
Willis, A. G. 1981, in *Optical Jets in Galaxies* (ESA SP-162), ed. B. Battrick and J. Mort (Paris: ESO), p. 71.
Willson, L. A., Garnavich, P., and Mattei, J. 1981, *Inf. Bull. Var. Stars*, No. 1961.

MOSHE ELITZUR: Department of Physics and Astronomy, University of Kentucky, Lexington, KY 40506

JAN M. HOLLIS: Code 630, Space Data and Computing Division, NASA/Goddard Space Flight Center, Greenbelt, MD 20771

MENAS KAFATOS: Department of Physics, George Mason University, Fairfax, VA 22030

ANDREW G. MICHALITSIANOS and F. YUSEF-ZADEH: Code 684, Laboratory for Astronomy and Solar Physics, NASA/Goddard Space Flight Center, Greenbelt, MD 20771